J Mater Sci (2017) 52:9922–9930

Polymers

Cotton fabric-based facile solar photocatalytic purification of simulated real dye wastes

Huawen Hu[1,2], Menglei Chang[1,*], Xiaowen Wang[2], and Dongchu Chen[1,*]

[1] College of Materials Science and Energy Engineering, Foshan University, Foshan 528000, Guangdong, China
[2] Institute of Textiles and Clothing, The Hong Kong Polytechnic University, Kowloon 999077, Hong Kong SAR, China

Received: 2 March 2017
Accepted: 17 April 2017
Published online: 25 April 2017

ABSTRACT

For the first time, this study presents solar photocatalytic processing of the real dye wastes remaining after finishing polyester/cotton (P/C) blends, rather than a pure organic dye solution as widely reported. A commonly used microencapsulation-based one-bath dyeing is investigated systematically, in order to simulate the real dyeing environment and to generate real dye wastes. The generated dye wastes are subsequently tackled by facile cotton fabric-based photocatalytic degradation involving a visible light-active TiO_2 photocatalyst under solar light. Importantly, such a TiO_2 photocatalyst is prepared without any calcination, doping, or coupling with plasmonic metal nanoparticles or narrow-band-gap semiconductors. As a result, the present visible light-responsive cotton fabric-based photocatalytic degradation of the simulated real dye wastes is expected to stimulate various industries for achieving simultaneous effective dyeing and processing of the dye wastes remained. This study also contributes to energy saving and environmental protection.

Introduction

Dyeing manufacturing is an essential procedure in many industries, but any dyeing processes leave dye wastes. Without proper treatment, the dye wastes are most likely to influx into the environment, causing many serious problems, such as aesthetic problems, and toxic threat to the aquatic living organisms and human beings [1]. As a result, facile but effective methods used to handle the dye wastes, remaining after dyeing, are urgently needed, so as to protect the environment and biological circles. Various methods have been employed to handle the dye wastes, such as adsorption, chemical precipitation, membrane filtration, biological treatment, and photocatalytic degradation [2–13], among which photocatalytic degradation under solar irradiation conditions is the most feasible way to realize the energy conservation and environmental protection. This is because of (1) exploitation of the inexhaustible, renewable solar energy [1] and (2) water and carbon dioxide as the final reaction products after the photocatalysis [14].

Due to the odourless, non-toxic and chemically stable properties of TiO_2-based photocatalysts, they are widely employed and deeply analysed for processing organic wastes [15]. However, TiO_2 possesses

Address correspondence to E-mail: mengleic@sina.com; cdcever@163.com

DOI 10.1007/s10853-017-1107-5

a large energy band gap and is insensitive to visible light which occupies a large part of solar light [16]. As a result, to make TiO_2 visible light-active is significant to harvest more solar energy for photocatalysis. This study explores visible light-responsive TiO_2 nanoparticles, without any complex calcination, doping, or coupling with plasmonic metal nanoparticles or narrow-band-gap semiconductors [17]. Unfortunately, TiO_2 particles down to nanoscale are extremely difficult to recycle. A support material is therefore needed to carry and immobilize these TiO_2 nanoparticles. In this study, a flexible cotton fabric is employed as the support to produce a fabric-based photocatalyst using a facile dip-pad-cure method [18], which is a traditional post-finishing process for textiles. The dipping process is to first adsorb the finishing agent, in this case TiO_2 nanoparticles, onto the cotton fabric, followed by padding under pressure to remove the excess TiO_2 nanoparticles without good adhesion to the cotton fabric and finally curing at high temperatures to immobilize TiO_2 nanoparticles on the cotton fabric. After the dip-pad-cure process, strong interfacial adhesion between the cotton fabric and TiO_2 nanoparticles is suggested to be formed, especially considering the hydrogen bonding interactions between the abundant hydroxyl groups on both the cotton fabric and the surface of TiO_2 nanoparticles. The prepared portable, flexible cotton fabric-based photocatalyst can then be easily recycled and reused, indicating little secondary environmental pollution as caused by TiO_2 nanoparticles, which can usually be observed when neat TiO_2 nanopowder is employed as the photocatalyst to handle the wastewater [19].

In this study, self-made real dye wastes, in dyeing popular polyester/cotton (P/C) blends, are used as the target to be tackled. For dyeing P/C blends, various dyeing parameters are also investigated systematically, so as to simulate the real dyeing environment and to generate the real dye wastes, rather than a pure organic dye pollutant as reported in most publications [20–22]. Here, a common microencapsulation-based one-bath dyeing method is employed for efficient dyeing and generating real dye wastes. This dyeing method involves the sustained release of microencapsulated disperse dye for dyeing polyester under high temperature and pressure conditions; cotton is simultaneously dyed with reactive dye in the dye bath, realizing effective one-bath dyeing of the P/C blends. Subsequently, the dye wastes remaining after the one-bath dyeing are handled by the cotton fabric-based solar photocatalysis.

Experimental

Materials

Titanium tetraisopropoxide (TTIP) of AR grade was supplied by Oriental Chemicals and Lab. Supplies Ltd. (Hong Kong SAR, China). All P/C blends (65/35, plain weave, specific density of 125 g/m^2) were supplied by Wujiang Textile Co. (China). The anionic dispersing agent NNO (polyoxyethylene octanol) and the nonionic penetrating agent JFC (sodium bis-naphthalenesulphonate) were provided by Gaoqiao Fine Chemicals Co. Ltd. (China). The Duisburg sodium sulphate (anhydrous sodium sulphate), caustic soda, sodium hydrosulphite, and soap flakes were provided by Shanghai Zhenxing Chemicals Co. Ltd. (China). All the chemicals used in the study were of reagent grade. CI microencapsulated disperse dye, Blue 79, was fabricated by ourselves (the molecular structure of the disperse dye Blue 79 is given in Fig. S1, Supporting Information (SI)). Polyurea microcapsules containing the disperse dye were prepared by an interfacial polymerization reaction in an emulsion form. Argazol Blue NF-BG (a reactive dye) was supplied by Shanghai Yayun Co. (China), which can be fixed under neutral pH and high-temperature conditions without alkali, thus being suitable for the one-bath dyeing of P/C blends. The pH buffering agent was also obtained from Shanghai Yayun Co. (China). All other chemicals were purchased from Sigma-Aldrich and used as received.

One-bath dyeing of P/C blends

The P/C blends were dyed in an IR dyeing machine (Rapid, Tai Wan) according to the one-bath dyeing profiles shown in Figs. S2 and S3 (SI) corresponding to the microcapsulation-related strategy and a conventional method without involving microcapsulation, respectively. The dosage of the ingredients used for making the dye bath, with microcapsulation involved, is presented in Table S1 of SI, and the other conventional one without involving microcapsulation is given in Table S2 (SI). Note that the dye bath, in both cases, was kept neutral. The dyeing substrate

was the P/C blends (65/35), with a size of 10×16 cm^2.

As for the conventional method without involving microcapsulation, after the dyeing process the colorized P/C bends were thoroughly washed through continuous rinsing, reduction clearing, rinsing, soaping, and rinsing to remove the dye stains from the colorized P/C fabric surface. The soaping process was carried out at 90 °C for 20 min, using 2.0 g/L of soap flakes at a liquor ratio of 1:20. The clearing process by reduction treatment was conducted at 85 °C for 15 min, with NaOH (2.0 g/L) and sodium hydrosulphite (2.0 g/L) at a liquor ratio of 1:20.

Regarding the present strategy with microcapsulation involved, the cleaning process is given as follows: once the temperature was cooled to 80 °C, the dyed samples were collected, followed by rinsing and soaping at 90 °C for 20 min, with 2 g/L of soap flakes at a liquor ratio of 1:20.

Synthesis of TiO_2 nanohydrosol

To fabricate the cotton fabric-based photocatalyst, TiO_2 nanohydrosol was first synthesized [17]. Briefly, TTIP was drop-added (one drop per second) into a mixed acid solution under vigorous mechanical stirring at 83 ~ 90 °C for 4 h, along with stepwise addition of deionized (DI) water, to realize the controlled hydrolysis of TTIP. The resulting milk-like sol was then cooled to 60 °C, leading to its increased fluid viscosity. The subsequent 15-h stirring resulted in transparent bluish sol, followed by cooling to room temperature and then ageing for 2 weeks to obtain the final hydrosol containing TiO_2 nanoparticles (10 wt%). The TiO_2 nanopowder was obtained by drying the prepared TiO_2 hydrosol at room temperature.

Fabrication of a cotton fabric-based photocatalyst

The as-prepared TiO_2 hydrosols were used to functionalize a cotton fabric through forming a thin coating of TiO_2 nanoparticles on the cotton fabric (white, woven), by dip-pad-cure processing, as commonly used to finish textile materials. The TiO_2 nanohydrosol with a 2% concentration was adopted to finish the cotton fabric, and the resultant finished cotton fabric had a wet pickup of 80%. The final mass ratio of dried cotton to the inorganic TiO_2 coating is 1/0.016 (g/g).

Photocatalytic degradation of simulated real dye wastes

After the dyeing and washing processes, the microcapsulated disperse dye was first removed from the dye bath by filtration, leaving most reactive dye as residual wastes to be tackled. The cotton-based photocatalyst, namely the TiO_2-functionalized cotton fabric (0.5 g), was cut into small pieces and then added into the residual dye bath (20.0 g). The dye bath with the cotton-based photocatalyst was then exposed to a source of simulated sunlight in a light fastness tester (XENOTEST ALPHA LM) according to the standard of ISO 105-B02:1988.

Recycling performance of the cotton fabric-based photocatalyst

Upon completion of the photocatalytic processing of the dye waste, a new cycle was consequently conducted according to the following steps: (1) recycling of the photocatalytically functionalized cotton fabrics by simply collecting them from the photocatalytic reaction solution; (2) thoroughly washing them with DI water followed by drying with the assistance of compressed gases at room temperature; (3) reusing the dried functionalized cotton fabrics in a new cycle with the same procedures mentioned above for the photocatalytic processing of the dye wastes remaining after the one-bath dyeing; and (4) repeating the above (1) to (3) until total five runs were completed.

Characterization

SEM observation was performed on a JSM-5600LV electron microscope (JEOL, Japan). The microcapsules were sprinkled onto a sample plate and were then sputter-coated with gold prior to examination. The colour yield (K/S) values of each sample were measured using a Datacolor SF600 instrument illuminated by a D65 LED. The photocatalytic degradation of the dye wastewater that leaves behind after the one-bath dyeing was monitored on an U-3310 UV/vis spectrophotometer at λ_{max} of 597 nm. The washing and rubbing fastnesses were determined according to the standards ISO/DIS 105-C03:1989 and ISO 105X-12:1993, respectively. The powder XRD

patterns were read on a Bruker D8 Advance X-ray diffractometer (Bruker AXS, Karlsruhe, Germany). TEM images coupled with SAED patterns were captured using a JEOL JEM-2011 TEM at an acceleration voltage of 100 kV. The specimen employed for TEM measurements was prepared by dropping a diluted TiO_2 nanohydrosol onto a silicon wafer, followed by drying at room temperature.

Results and discussion

The main content of this study is presented in Fig. 1, primarily including the microencapsulation-related one-bath dyeing of P/C blends, generation of real dye wastes, fabrication of a cotton fabric-based photocatalyst with a hydrosol containing visible light-responsive TiO_2 nanoparticles, and final processing of the real dye wastes by the cotton fabric-based photocatalytic degradation under simulated solar light.

SEM observation of the prepared microcapsules containing the disperse dye Blue 79 is shown in Fig. S4 (SI). The microcapsules can be well dispersed in the water media, facilitating the one-bath dyeing process. Various dyeing parameters are systematically investigated for the one-bath dyeing, as shown in Fig. 2. Figure 2a depicts plots of K/S value of the dyed P/C blends as a function of the liquor ratio for the systems involving conventional one-bath dyeing and microencapsulation-related one-bath dyeing. As the liquor ratio increases, the K/S value of the dyed P/C blends is lowered for both the systems, but the conventional system is obviously more vulnerable with the change of the liquor ratio, as judged by the a much larger K/S value dropping tendency with decreasing the liquor ratio. This implies the more stable and viable microencapsulation-related one-bath dyeing. Except at the liquor ratio of 1:10, impressive levelling of the dyed P/C blends could be observed for all other liquor ratios as investigated. As a result, the optimal liquor ratio for the present one-bath dyeing with microencapsulated disperse dye can be determined as 1:20. With the fixed ratio, the influence of the dyeing temperature on the K/S value of the dyed P/C blends is then investigated (Fig. 2b). Dye species and textile substrates are also varied, including single reactive dye for dyeing a pure cotton substrate, single microencapsulated disperse dye for dyeing a pure polyester substrate, and combined reactive dye with microencapsulated disperse dye for dyeing P/C blends. The K/S value of the dyed cotton using the reactive dye reaches the maximum at 100 °C and thereafter levels off. In comparison, the K/S value of the dyed polyester reaches the maximum at 130 °C, which is larger than that of the dyed cotton. The K/S values of dyed P/C blends at different dyeing temperatures just lie between those of dyed polyester and dyed cotton. It seems that the optimal dyeing temperature for the P/C blends using

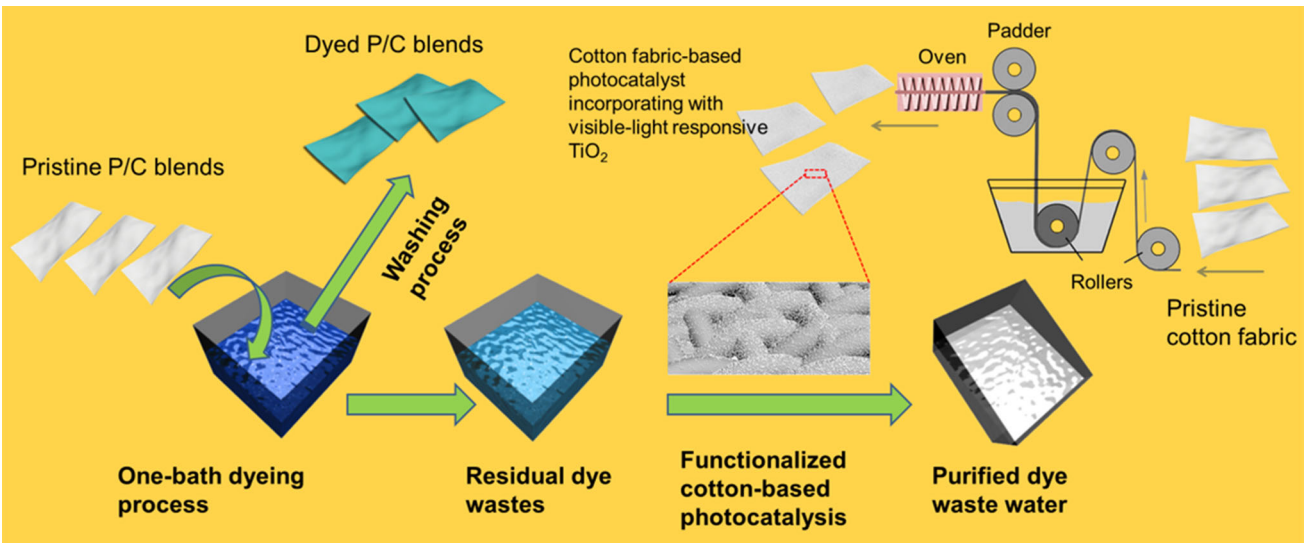

Figure 1 Schematic presentation of the main content of the present study, including the microencapsulation-related one-bath dyeing of P/C blends, generation of dye wastes, incorporation of the TiO_2 nanoparticles onto the cotton fabric, and cotton fabric-based solar photocatalytic degradation of the simulated real dye wastes.

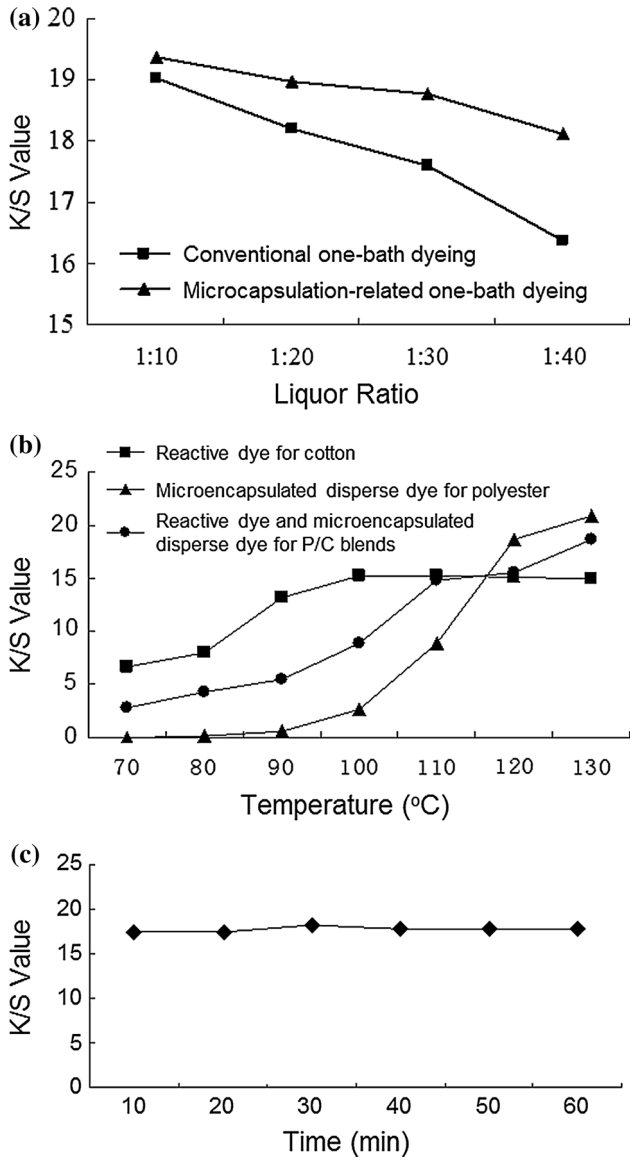

Figure 2 Optimizing the dyeing parameters to simulate real dyeing processing and to generate real dye wastes. **a** Investigation of the influence of the liquor ratio on the K/S value of the dyed P/C blends, and comparison of the dyeing effect between the conventional one-bath dyeing and the present microencapsulation-related one-bath dyeing. **b** Plots of the K/S value of the dyed fabric as a function of the dyeing temperature for three different dyeing systems, i.e. single reactive dye for pure cotton, single microencapsulated disperse dye for pure polyester, and combined reactive dye with microencapsulated disperse dye for P/C blends. **c** Plot of the K/S value of the dyed P/C blends as a function of dyeing time, in this case heat preservation time, for the one-bath dyeing, with microencapsulated disperse dye coupled with reactive dye.

the microencapsulated disperse dye coupled with reactive dye is around 130 °C, although the K/S value changes much more slowly at temperatures of higher than 110 °C. Finally, we examine the impact of heat preservation time on the K/S value of the dyed P/C blends, with a fixed liquor ratio of 1:20 and heat preservation at 130 °C, as shown in Fig. 2c. The K/S value keeps almost constant with varying heat preservation time, and 30 min appears sufficient to produce a high K/S value, excellent levelness, and impressive fastness properties. For more detailed information on the dyeing test results, Tables S3 and S4 (SI) can be referred to. The comprehensive properties of the dyed P/C blends prepared by the present microencapsulation-related technology are found to be superior to that for the conventional dyeing method. Therefore, the former is more desirable for producing high-quality colorized P/C blends. After the microencapsulation-related dyeing process, dye wastes are collected for the following photocatalytic degradation.

Facile cotton fabric-based solar photocatalysis is employed to deal with the simulated real dye wastes. The visible light-responsive TiO_2 nanohydrosol was first prepared, with characterization results presented in Fig. 3. A photoimage of the prepared TiO_2 nanohydrosol is shown in Fig. 3a, which shows good dispersibility and uniformity. Figure 3b gives the XRD pattern of the prepared TiO_2 nanoparticles, confirming their dominant anatase crystallization phase (JCPDS No. 21-1272), even though a trace amount of brookite TiO2 can also be evidenced from the XRD band at $\sim 30.8^{o}$, corresponding to the brookite (121) plane [23]. According to the Scherrer equation and the anatase (101) reflection, the crystallite size of TiO_2 nanoparticles is calculated to be approximately 4.82 nm. The broadening of the diffraction peaks is also an indication of a small size of the TiO_2 nanoparticles on average. Based on the Rietveld analysis using pseudo-Voigt model for peak fitting (Fig. S5 of SI), an average crystal size is also estimated to be around 4.7 nm, very close to the one calculated by the Scherrer equation. Figure 3c presents a TEM image coupled with a SAED pattern (see inset) of the TiO_2 nanoparticles (as highlighted by red circles), which have an average size of about 4.05 nm, close to that estimated from the XRD pattern. A crystalline lattice spacing of $\sim$0.36 nm (Fig. 3c), corresponding to (101) crystallographic plane of anatase TiO_2, also confirms the presence of the main anatase phase [24]. The energy band gap of our synthesized TiO_2 nanoparticles is around 2.98 eV, as calculated from the Tauc plot of transformed Kubelka–Munk

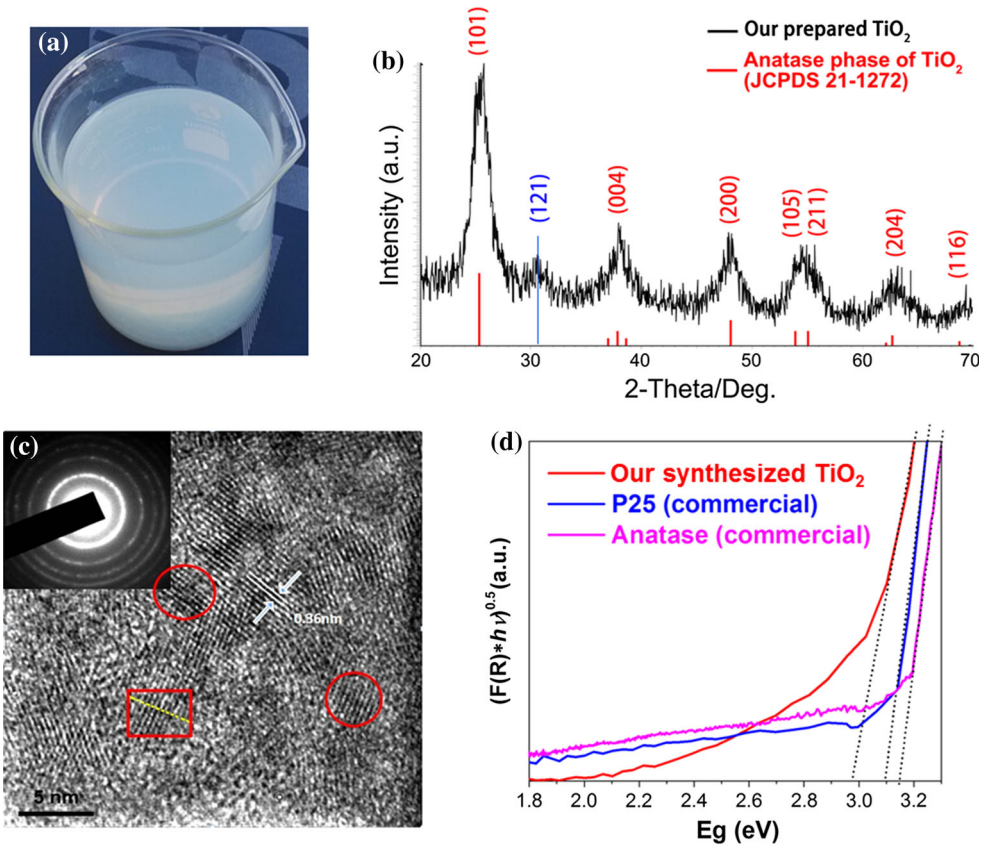

Figure 3 Characterization of the synthesized TiO_2. **a** A photoimage of the synthesized TiO_2 nanohydrosol. **b** XRD pattern of the prepared TiO_2 nanoparticles. **c** TEM image of the TiO_2 nanoparticles; inset shows the corresponding SAED pattern. **d** Tauc plots of transformed Kubelka–Munk function versus the energy of light for different types of TiO_2 including the as-synthesized visible light-responsive TiO_2, commercial P25, and commercial TiO_2 with the pure anatase phase.

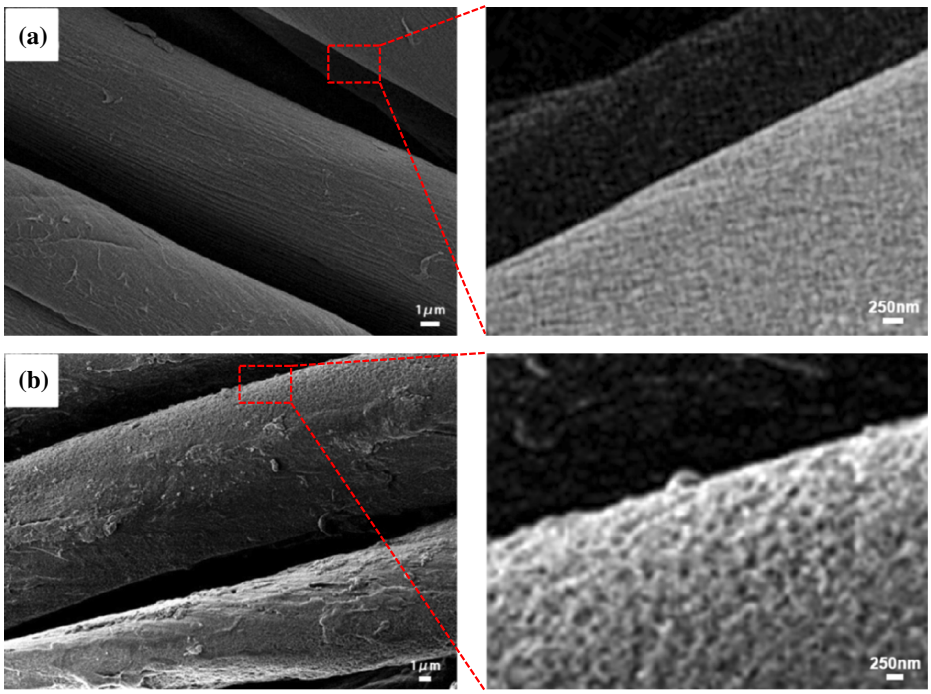

Figure 4 SEM observation of the bare cotton fabric **(a)** and cotton fabric-based photocatalyst **(b)**; the corresponding magnified SEM images are presented in the *right side*.

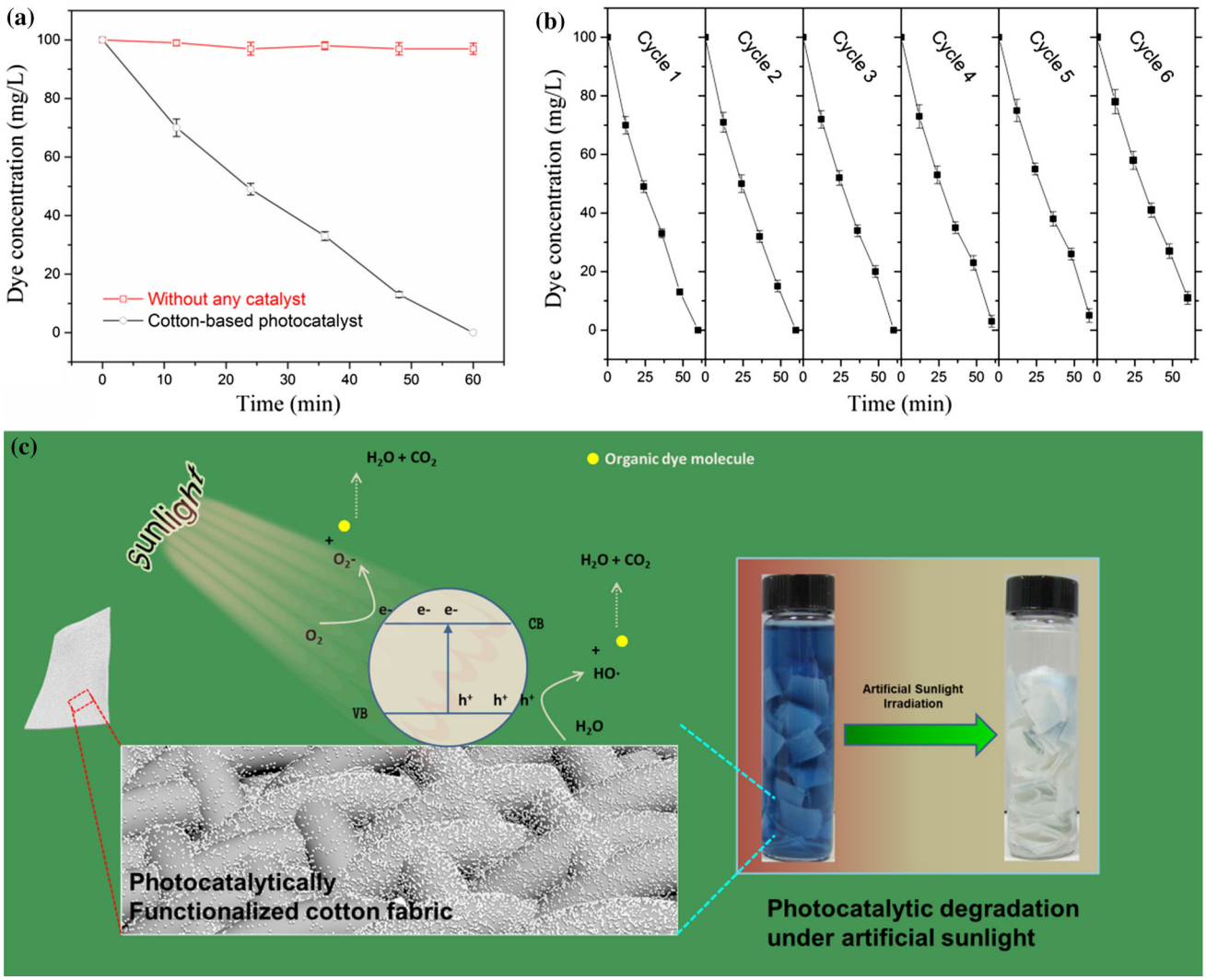

Figure 5 Cotton fabric-based solar photocatalytic degradation of the simulated real dye wastes, as generated after the microencapsulation-related one-bath dyeing process. **a** Solar photocatalytic degradation of the simulated real dye wastes using the cotton fabric-based photocatalyst, along with the control test without any photocatalysts. **b** Recycling performance of the cotton fabric-based photocatalyst through total six runs of repeated usage. **c** An understanding of the cotton fabric-based solar photocatalysis mechanism.

function versus the energy of light (Fig. 3d), being smaller than 3.15 and 3.10 eV for commercial anatase and P25, respectively.

To coat the TiO_2 nanoparticles onto a cotton fabric, a dip-pad-cure method was adopted using the prepared TiO_2 nanohydrosol. The schematic presentation of the dip-pad-cure process is also given in Fig. S6 of SI. SEM observation of the bare cotton fabric and the TiO_2 nanoparticles-finished cotton fabric is shown in Fig. 4a, b, respectively. Attributed to the hydrogen bonding interactions between the abundant hydroxyl groups on both the cotton fabric and the surface of the TiO_2 nanoparticles, strong interfacial interactions between the cotton fabric and the TiO_2 nanoparticles are suggested to be formed. From Fig. 4b, a TiO_2 coating layer, with roughness, can be observed on the cotton fabric surface after the dip-pad-cure finishing process, in contrast to the smooth surface of the bare cotton fabric (Fig. 4a), thus evidencing the fine incorporation of TiO_2 nanoparticles onto the cotton fabric.

With the cotton fabric-based photocatalyst, processing the real dye wastes left behind after the one-bath dyeing is thereafter carried out (Fig. 5). The dye wastes can be efficiently purified by simulated solar irradiation for only 60 min. By contrast, in the

absence of the cotton-based photocatalyst, the solar light irradiation only generates a little impact on the dye wastes (Fig. 5a). The recycling performance of the cotton fabric-based photocatalyst was also evaluated, and total six runs of repeated usage were performed (see Fig. 5b). It shows impressive recycling performance; after six runs of repeated usage, only a little degradation of the photocatalysis performance can be detected in spite of an intense washing procedure involved in each reuse cycle. We ascribe the stable cotton fabric-based photocatalytic degradation of the dye wastes to the strong interactions between the visible light-responsive ultra-small TiO_2 nanoparticles and cotton fabric base, as a result of the hydrogen bonding interactions between the hydroxyls on the surface of the TiO_2 nanoparticles and the hydroxyls of the cotton fabric. The mechanism behind the highly effective solar-light-driven photocatalytic degradation of the real dye wastes is described as follows: the solar light first drives promotion of the electrons from the valence band (VB) to the conduction band (CB), leaving an equal number of holes in the VB. Both photogenerated electrons and holes can react with surrounding species such as oxygen and water, respectively, to produce reactive oxygen species (ROS) that subsequently scavenge the organic dye species, which leads to the final production of water and carbon dioxide, as schematically shown in Fig. 5c and also reported elsewhere [25].

Conclusions

This study investigates solar-light-driven photocatalytic degradation of real dye wastes remaining after dyeing the popular P/C blends with a cotton fabric-based photocatalyst. Such a portable, flexible photocatalyst is prepared by immobilizing visible light-sensitive TiO_2 nanoparticles onto the cotton fabric, which shows satisfactory recycling and reuse performance, most likely resulting from the strong interfacial interactions between the TiO_2 nanoparticles and the cotton fabric. Therefore, the work presented here will bring a certain economic value to various industries, especially those involving colouration and finishing of textiles and related materials. This work is also expected to contribute to energy saving and environmental protection.

Acknowledgements

The authors greatly appreciate the special funding project of the technical innovation of Foshan city (2014AG10009), the self-innovation promotion project of the universities in Guangdong Province (2015KQNCX178), and research centre project of engineering technology of Foshan City (2014GA000355).

Electronic supplementary material: The online version of this article (doi:10.1007/s10853-017-1107-5) contains supplementary material, which is available to authorized users.

References

[1] Hu H, Xin JH, Hu H, Wang X, Miao D, Liu Y (2015) Synthesis and stabilization of metal nanocatalysts for reduction reactions—a review. J Mater Chem A 3:11157. doi:10.1039/c5ta00753d

[2] Parmar KR, Patel I, Basha S, Murthy ZVP (2014) Synthesis of acetone reduced graphene oxide/Fe3O4 composite through simple and efficient chemical reduction of exfoliated graphene oxide for removal of dye from aqueous solution. J Mater Sci 49:6772. doi:10.1007/s10853-014-8378-x

[3] Bumajdad A, Madkour M, Abdel-Moneam Y, El-Kemary M (2013) Nanostructured mesoporous Au/TiO2 for photocatalytic degradation of a textile dye: the effect of size similarity of the deposited Au with that of TiO2 pores. J Mater Sci 49:1743. doi:10.1007/s10853-013-7861-0

[4] Hu H, Xin JH, Hu H, Wang X (2015) Structural and mechanistic understanding of an active and durable graphene carbocatalyst for reduction of 4-nitrophenol at room temperature. Nano Res 8:3992. doi:10.1007/s12274-015-0902-z

[5] Hu H, Xin JH, Hu H (2014) PAM/graphene/Ag ternary hydrogel: synthesis, characterization and catalytic application. J Mater Chem A 2:11319. doi:10.1039/c4ta01620c

[6] Hu H, Xin JH, Hu H, Chan A, He L (2013) Glutaraldehyde–chitosan and poly (vinyl alcohol) blends, and fluorescence of their nano-silica composite films. Carbohydr Polym 91:305. doi:10.1016/j.carbpol.2012.08.038

[7] Hu H, Wang X, Miao D et al (2015) A pH-mediated enhancement of the graphene carbocatalyst activity for the reduction of 4-nitrophenol. Chem Commun 51:16699. doi:10.1039/c5cc05826k

[8] Hu H, Allan CCK, Li J et al (2014) Multifunctional organically modified graphene with super-hydrophobicity. Nano Res 7:418. doi:10.1007/s12274-014-0408-0

[9] Hu H-W, Xin JH, Hu H (2013) Highly efficient graphene-based ternary composite catalyst with polydopamine layer and copper nanoparticles. ChemPlusChem 78:1483. doi:10.1002/cplu.201300124

[10] Hu H, Xin J, Hu H, Wang X, Lu X (2014) Organic liquids-responsive β-cyclodextrin-functionalized graphene-based fluorescence probe: label-free selective detection of tetrahydrofuran. Molecules 19:7459. doi:10.3390/molecules19067459

[11] Xue Z, Zhao S, Zhao Z, Li P, Gao J (2016) Thermodynamics of dye adsorption on electrochemically exfoliated graphene. J Mater Sci 51:4928. doi:10.1007/s10853-016-9798-6

[12] Zhang J, Xiao H, Yang Y (2014) Preparation of hemicellulose-containing latex and its application as absorbent toward dyes. J Mater Sci 50:1673. doi:10.1007/s10853-014-8728-8

[13] Scaglione F, Battezzati L (2015) Metastable microstructures containing zero valent iron for fast degradation of azo dyes. J Mater Sci 50:5238. doi:10.1007/s10853-015-9071-4

[14] Chong MN, Jin B, Chow CWK, Saint C (2010) Recent developments in photocatalytic water treatment technology: a review. Water Res 44:2997. doi:10.1016/j.watres.2010.02.039

[15] Qu X, Xie D, Gao L, Cao L, Du F (2014) Synthesis and characterization of TiO2/WO3 composite nanotubes for photocatalytic applications. J Mater Sci 50:21. doi:10.1007/s10853-014-8441-7

[16] Liu E, Fan J, Hu X et al (2014) A facile strategy to fabricate plasmonic Au/TiO2 nano-grass films with overlapping visible light-harvesting structures for H2 production from water. J Mater Sci 50:2298. doi:10.1007/s10853-014-8793-z

[17] Wang X, Hu H, Yang Z, Kong Y, Fei B, Xin JH (2015) Visible light-active sub-5 nm anatase TiO2 for photocatalytic organic pollutant degradation in water and air, and for bacterial disinfection. Catal Commun 72:81. doi:10.1016/j.catcom.2015.09.014

[18] Kong Y, Liu Y, Xin JH (2011) Fabrics with self-adaptive wettability controlled by "light-and-dark". J Mater Chem 21:17978. doi:10.1039/c1jm12516h

[19] Gondikas AP, Fvd Kammer RB, Reed S Wagner, Ranville JF, Hofmann T (2014) Release of TiO_2 Nanoparticles from sunscreens into surface waters: a one-year survey at the old Danube recreational lake. Environ Sci Technol 48:5415. doi:10.1021/es405596y

[20] Han J, Zhu G, Hojamberdiev M, Peng J, Liu P (2015) Synergetic effects of surface adsorption and photodegradation on removal of organic pollutants by Er^{3+}-doped BiOI ultrathin nanosheets with exposed 001 facets. J Mater Sci 51:2057. doi:10.1007/s10853-015-9516-9

[21] Dinari M, Momeni MM, Ghayeb Y (2016) Photodegradation of organic dye by ZnCrLa-layered double hydroxide as visible-light photocatalysts. J Mater Sci Mater Electron 27:9861. doi:10.1007/s10854-016-5054-8

[22] Cao QW, Zheng YF, Yin HY, Song XC (2016) A novel AgI/AgIO3 heterojunction with enhanced photocatalytic activity for organic dye removal. J Mater Sci 51:4559. doi:10.1007/s10853-016-9769-y

[23] Zhao H, Liu L, Andino JM, Li Y (2013) Bicrystalline TiO2 with controllable anatase–brookite phase content for enhanced CO2 photoreduction to fuels. J Mater Chem A 1:8209. doi:10.1039/c3ta11226h

[24] Bykkam S, Rao KV, Naresh Kumar R, Shilpa Chakra C, Dayakar T (2016) Few-layered graphene decked with TiO2 nano particles by ultrasonic assisted synthesis and its dye-sensitized solar cell application. J Mater Sci Mater Electron 27:12574. doi:10.1007/s10854-016-5388-2

[25] Han F, Kambala VSR, Srinivasan M, Rajarathnam D, Naidu R (2009) Tailored titanium dioxide photocatalysts for the degradation of organic dyes in wastewater treatment: a review. Appl Catal A Gen 359:25. doi:10.1016/j.apcata.2009.02.043